Grasp Invariance*

Alberto Rodriguez and Matthew T. Mason

February 1, 2012

Abstract

This paper introduces a principle to guide the design of finger form: invariance of contact geometry over some continuum of varying shape and/or pose of the grasped object in the plane. Specific applications of this principle include scale-invariant and pose-invariant grasps. Under specific conditions, the principle gives rise to spiral shaped fingers, including logarithmic spirals and straight lines as special cases. The paper presents a general technique to solve for finger form, given a continuum of shape or pose variation and a property to be held invariant. We apply the technique to derive scale-invariant and pose-invariant grasps for disks, and we also explore the principle's application to many common devices from jar wrenches to rock-climbing cams.

1 Introduction

What principles should guide the design of finger form? It depends on context—the specific application, the hand design philosophy, and in particular on the function assigned to the fingers. In this paper we explore the possible role of fingers in adapting to variations in object shape and pose. One common design approach is to adapt to those variations by active control of several actuators per finger. But for simpler hands, with one actuator per finger, or even one actuator driving several fingers, the job of gracefully adapting to shape and pose variations may fall on the finger form. This work explores grasp invariance over shape and/or pose variation as a principle for finger form design.

We begin by proposing a geometry problem:

> *Scale-invariant contact problem*: Given $\mathcal{O}$ an object shape in the plane, p a point on the boundary of $\mathcal{O}$, and c the location of the finger's revolute joint, find the finger shape that makes contact at p despite scaling of $\mathcal{O}$ (Figure 1).

A solution to the previous problem yields a finger shape that preserves contact location as well as contact normal with the scale of the object. As a consequence, many properties governing the mechanics of grasping and manipulation are also preserved. For example, we will see in Section 5.1 that if $\mathcal{O}$ is a disk in the palm of a two-fingered hand, the solution to

Alberto Rodriguez and Matthew T. Mason are with the Robotics Institute at Carnegie Mellon University, 5000 Forbes Avenue, Pittsburgh, PA 15213, <albertor@cmu.edu , matt.mason@cs.cmu.edu>

An earlier version of this paper appeared in proceedings of the 2010 Workshop on Algorithmic Foundations of Robotics (WAFR).

*The International Journal of Robotics Research Vol. 31, No. 2 February 2012, pp. 237-249.

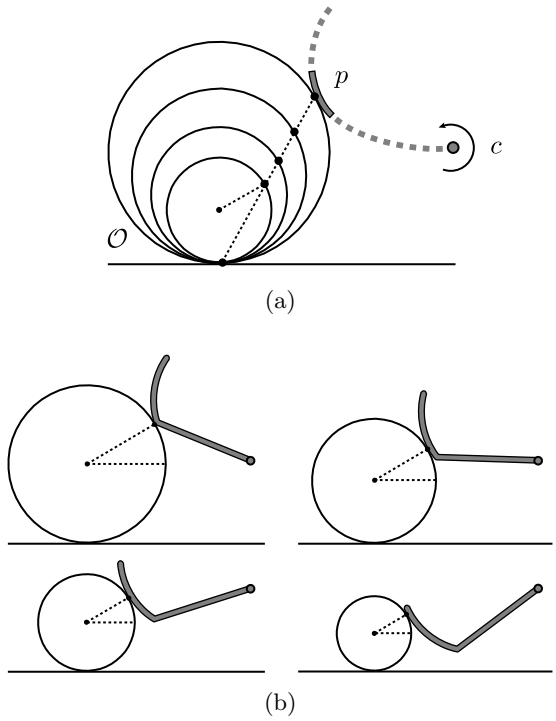

Figure 1: The scale-invariant contact problem (a), solved in Section 3.2, yields a finger shape whose contact with the object $\mathcal{O}$ is preserved for different sizes of $\mathcal{O}$ (b).

the scale-invariant contact problem yields identical equilibrium grasps despite variations in the scale of the disk, assuming the object is static during the grasping process.

This paper generalizes the scale-invariant contact problem, and explores its implications for finger design in grasping and fixturing problems. Scale-invariant contact is just one example of a broader class of problems where a continuum of constraints guides the design of finger shape. In the specific case of scale invariance, the set of constraints is generated by scaling the object. We present in this paper different sets of transformations of the object yielding finger forms optimized for a variety of tasks.

In Section 3 we show how, under certain conditions, the problem can be mathematically formulated and admits a unique solution as an integral curve of a vector field. In Section 4 we find the analytical expression of the integral curve for the most simple and common cases. The integration yields spiral shaped fingers—in special cases, a logarithmic spiral, a shape long noted for its scale invariant properties [15]. Finally, in Section 5 and Section 6, we show that the principle applies to fixture and finger designs seen in many common devices from jar wrenches to rock-climbing cams.

2 Related Work on Finger Design

This paper grew out of our interest in simple hands, focused on enveloping grasps of objects with uncertain pose and shape [13]. The traditional approach to grasping uses knowledge of object geometry and grasp mechanics to plan for contact points. In this context the details of

phalange form are of little consequence, since only the tip of the finger is involved in the grasp.

Simple hands, however, do not necessarily have the required capabilities to plan for contact points. The actual forms of the phalanges and the palm become important when the locations of contacts are not carefully planned and controlled. Simple hands adapt to varying shapes and poses by the emergent interaction of hand with object, rather than by actively driving the hand shape to conform to a known object shape and pose.

Several other approaches are evident in previous hand design literature. The enveloping grasps we employ are contrasted with fingertip grasps, more suited to the traditional approach to grasping. The dichotomy between enveloping and fingertip grasps corresponds roughly to the distinction between power and precision grasps in Cutkosky and Wright's grasp taxonomy [8].

While much of the analysis of grasp has focused on local stability and in-hand manipulation with fingertip grasps [5], hand design research has explored various grasp types more broadly. The work leading to the design of the Barrett Hand [19, 18, 1] explored a single finger probe, a pinch grasp , both cylindrical and spherical enveloping grasps, a two-fingered fingertip grasp, and a hook grasp. The design of the DLR-II likewise was guided by the desire to produce both power and precision grasps [7].

Unlike the work cited so far, our approach does not change the shape of the fingers to adapt to an object pose or shape. Instead, adaptation emerges from the interaction of fixed finger shapes with the object. In that respect the closest work is Trinkle and Paul's [17] work on enveloping grasps, Dollar and Howe's [10] work on hands with compliantly coupled joints, and Theobald et al.'s [14] design of a gripper for acquiring rocks. Still, none of the above focus on the actual finger form. Dollar and Howe [9] surveyed 20 different designs of compliant and underactuated hands, and all employ cylindrical or straight fingers, occasionally employing some additional shape features, but with no particular principle described to guide their design.

Our interest in shape design has some commonalities with work on algorithmic approaches to the design of chamfers and traps. Whitney, Gustavson and Hennessey [20] proposed procedures to design straight and curved chamfers to aid in the assembly of rigid parts. Berretty et al. [4] reasoned about the geometry of object/trap interaction in vibratory bowl feeders for object filtering.

Work on fence design in the context of parts feeding [12, 21, 3] is also relevant to this paper. When objects on a conveyor make contact with a fence, the resulting interaction can reduce uncertainty in object pose. Because of frictional uncertainty, as the parts lose contact with the fence, there is always some remaining uncertainty in object pose. Brokowski, Peshkin and Goldberg [6] designed curved fence tails to minimize the effect of frictional uncertainty. The technique proposed in [6] for fence tail design has some similarities with the recipe we provide in this paper to solve for finger shape.

Still in the context of parts feeding, Zhang and Goldberg [22] systematized the design of parallel jaw grippers for alignment of parts in the vertical plane. They proposed to use four gripper point contacts to passively align the part in the vertical plane as the jaws close.

The closest work to this paper is found not in robotics research, but in the design of various tools and hardware. All the devices in Figure 2 adapt to shape and pose variations without changing their internal shape. Instead, the adaptation arises from their designed curvature. In the cases of the rock-climbing cam [11] and the anti-kickback device [2] the shape was derived mathematically. The others, to our knowledge, are the product of human intuition. In Section 6 we analyze their shape under the grasp invariance principle.

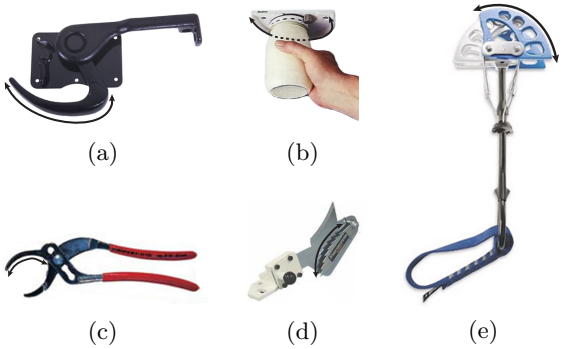

Figure 2: Curved shapes used in: (a) Truck door lock; (b) Jar opener; (c) Anti-kickback device for table saw; (d) Pliers; (e) Climbing cam.

3 Problem Formulation

In this section we generalize the formulation of the scale-invariant contact problem proposed in the introduction by considering now an arbitrary continuum of transformations of the object $\mathcal{O}$. As in the original problem, the interest lies in designing a finger that makes contact with $\mathcal{O}$ at a given point p, and preserves the contact geometry with respect to the set of transformations.

Let $\mathcal{H}(t, s)$ be a parametrization of the object boundary for the continuum of transformations, where s is the transformation parameter and t the boundary parameter. For any given value of the transformation parameter s, $h_s(t) = \mathcal{H}(t, s)$ parametrizes the boundary of the transformed object $\mathcal{O}$, with $h_s(0)$ mapping to the desired contact point p. Under this formulation, we generalize the scale-invariant contact problem as:

> *Invariant contact problem*: Given $\mathcal{O}$ an object shape in the plane, $\mathcal{H}(t, s)$ a continuous parametrization of a set of transformations of the object, and c the location of the finger's revolute joint, find the finger shape that makes first contact with the object at $\mathcal{H}(0, s)$ for all s.

Locally, requiring the finger to contact the object at p constrains the finger slope: finger and object must be tangent. In the following section we show that this interpretation leads to a reformulation of the problem in terms of vector fields.

3.1 Local Formulation of the Problem

Let *contact curve* $\mathcal{L}(s) = \mathcal{H}(0, s)$ describe the locus of the contact point p with the transformation of the object, and let *contact vector* $\mathcal{V}(s) = \frac{\partial \mathcal{H}(t,s)}{\partial t}|_{t=0}$ be the tangent to the object along the contact curve, as in Figure 3.

Every instance of the object corresponds to a point in the contact curve $\mathcal{L}$, for which the invariant contact problem imposes a constraint on the slope of the finger: it must be tangent to the contact vector $\mathcal{V}$; and a constraint on its curvature: the curvature of finger and object need to comply with each other so that there is no interpenetration. We will see in Section 3.3 that the curvature constraints are key to decide whether the invariant contact problem has a solution or not. We proceed in this section by showing how the set of slope constraints fully defines the finger form.

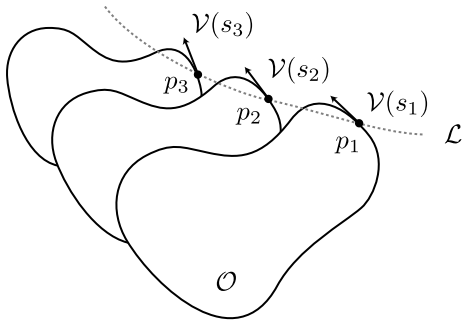

Figure 3: The transformation of the object $\mathcal{O}$ defines the contact points $p_i = \mathcal{H}(0, s_i)$ and with them, the contact curve $\mathcal{L}$ and the contact vector $\mathcal{V}$.

If we overlook the possibility of interpenetration between finger and object, the local version of the invariant contact problem formulates as:

> *Local invariant contact problem*: Given $\mathcal{O}$ an object shape in the plane and a parametrized set of transformations for which $\mathcal{L}$ is the contact curve and $\mathcal{V}$ the contact vector, and c the location of the finger's revolute joint, find the finger shape that always crosses the contact curve tangent to the contact vector.

Every point in the contact curve $\mathcal{L}$ yields a tangential constraint at a specific point along the finger. The map between points in the contact curve and points along the finger must be injective, since the slope of the finger cannot satisfy two different constraints simultaneously. To formulate that requirement we introduce the scalar function $r(s)$, the distance between a point in the contact line $\mathcal{L}$ and c, the center of rotation of the finger.

As illustrated in Figure 4a, while the finger rotates, each tangential constraint is propagated along an arc of radius $r(s)$ and center c (parallel transport of the contact vector $\mathcal{V}(s)$). When applying the same construction to the entire set of constraints, as in Figure 4b, it follows that the scalar function $r(s)$ must be strictly monotonic, otherwise two different points along the contact line could possibly impose two different slope constraints along the same concentric arcs. If it is the case that $r(s)$ reaches an extremum, the map between points in the contact curve and points along the finger will not be injective and the invariant contact problem will impose inconsistent constraints.

In practice, given a parametrized transformation $\mathcal{H}(t, s)$ of the object and its correspondent contact curve, we avoid inconsistent constraints by restricting the synthesis process to a section of the contact curve where $r(s)$ is strictly monotonic, Figure 5. We will refer to a problem that avoids inconsistent constraints as a *proper problem.*

If we have a proper problem, the parallel transport of the contact curve and contact vector along concentric arcs yields a vector field $\mathcal{F}$ defined on an annulus in the plane. By construction, any integral curve of $\mathcal{F}$ must satisfy all contact curve constraints, hence it should be a solution to the local invariant contact problem.

We will see in Section 3.2 that the set of tangential constraints fully defines the finger form. In Section 3.3 we argue that smoothness of the contact curve as well as the travel of the contact vector is enough to guarantee the existence of solution to the local invariant contact problem.

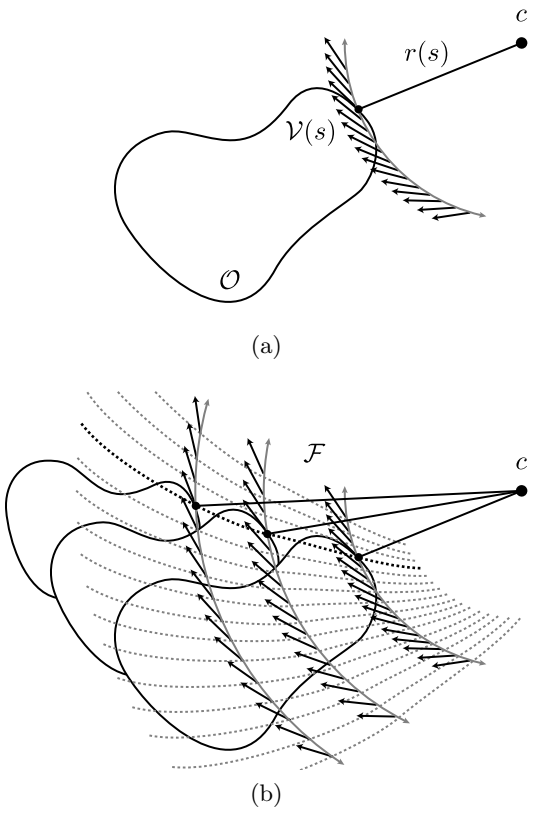

Figure 4: (a) Parallel transport of $\mathcal{V}(s)$ radially from c. (b) Extending the same construction to the entire set of tangential constraints gives us the vector field $\mathcal{F}$.

Finally, we discuss when a solution to the local invariant contact problem is also a solution to the more restrictive invariant contact problem.

3.2 General Solution Recipe

The derivation in the previous section suggests a three step general procedure for obtaining the shape of the finger:

1. Given an object $\mathcal{O}$ and a parametrized transformation $\mathcal{H}(t, s)$, construct the contact curve $\mathcal{L}$ and the contact vectors $\mathcal{V}$.

2. Obtain the vector field $\mathcal{F}$, by rotating $\mathcal{L}$ and $\mathcal{V}$ around the rotation center c.

3. Find the shape of the finger as an integral curve of $\mathcal{F}$.

Figure 6 shows an example of the procedure applied to the original scale-invariant contact problem for a disk-shaped object resting in a planar palm. When scaling the disk, the contact curve $\mathcal{L}$ becomes a line and the contact vector $\mathcal{V}$ is constant along $\mathcal{L}$.

The continuous set of transformations $\mathcal{H}(t, s)$ induces a continuous set of tangential constraints. Assuming that we have a proper problem, the vector field is well defined in a contin-

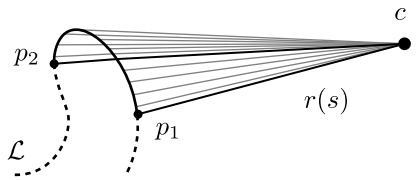

Figure 5: Example of maximal section of the contact curve $\mathcal{L}$ for which $r(s)$ is strictly monotonic. The minimum value of $r(s)$ is chosen at p_1. The value of r increases with the contact curve until reaching p_2, where an extremum prevents a further extension.

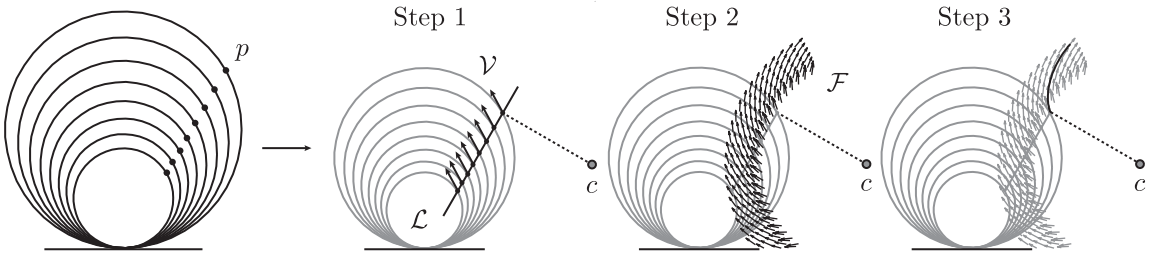

Figure 6: Step by step execution of the general recipe to obtain the form of the finger for the scale-invariant contact problem. Step 1: Construction of the contact curve $\mathcal{L}$ and contact vector $\mathcal{V}$. Step 2: Generation of the vector field $\mathcal{F}$. Step 3: Integral curve of $\mathcal{F}$.

uum of the space, and, hence, the finger form is fully defined. In the next section we see that the existence of the integral curve is guaranteed provided some regularity of $\mathcal{H}$.

3.3 Existence and Feasibility of Solution

It follows from the previous sections that the solution to the local invariant contact problem is subject to the existence of an integral curve of the vector field $\mathcal{F}$. We rely on the theorem of existence and uniqueness of maximal integral curves [16] for that.

Theorem 1 (Existence and Uniqueness of Maximal Integral Curves) *Let X be a smooth vector field on an open set $U \in \mathbb{R}^{n+1}$ and let $p \in U$. Then there exists a unique and maximal integral curve $\alpha(t)$ of X such that $\alpha(0) = p$.*

By virtue of Theorem 1 the existence of the integral curve depends on the smoothness of the vector field $\mathcal{F}$. If the contact curve $\mathcal{L}$ is smooth and $\mathcal{V}$ changes smoothly along it, the vector field will also be smooth, since the parallel transport along concentric arcs is a continuous and differentiable operation. If that is the case, the solution to the local invariant contact problem is guaranteed to exist for the restricted interval of values of s where the problem is a proper problem.

For this to also be a solution to the invariant contact problem, we need to check that it does not induce interpenetration between finger and object. There are two types of interpenetration that tend to happen in the vicinity of convexities of the object:

- **Local interpenetration**: As mentioned in the beginning of Section 3.1, being tangent

to the object is not enough to guarantee that locally object and finger contact at p, Figure 7a. Their curvature must comply with each other.

- **Global interpenetration**: Even if curvatures of finger and object comply locally, other sections of the finger might collide with the object, Figure 7b.

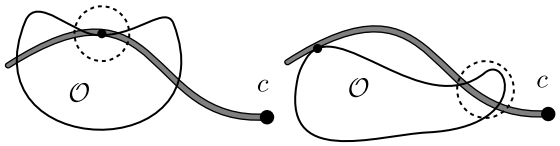

(a) (b)

Figure 7: Examples of interpenetration between finger and object. In both examples, the finger contacts the object at the desired location (black dot) with the right slope. However, that is not enough for the finger to be a solution to the invariant contact problem. (a) Curvatures of finger and object are not adequate to prevent local interpenetration. (b) Even with adequate curvatures, interpenetration can happen with the rest of the object $\mathcal{O}$.

Given that the tangential constraints fully define the finger form, the solution to the contact invariant problem is either that same finger form or no solution at all, when it implies any form of interpenetration. Hence, we should add a fourth step to the general solution recipe in Section 3.2, where we check for the feasibility of the solution yielded by the integration of the vector field. If we are given the freedom to play with some of the givens of the problem, such as the contact point p or the location of the rotation center of the finger c, dealing with interpenetration becomes a design issue.

4 Analytic Solution

The recipe in Section 3.2, along with numerical integration, provides a method to find the finger form for any given object $\mathcal{O}$ and any parametrized transformation $\mathcal{H}(t, s)$. In this section we find the analytical expression of the finger shape for some specific cases, namely when the contact curve is a line and the contact vector is constant along it. Note that this includes the cases of scaling of the object, translation of the object, or any linear combination of both.

Let (x, y) and (r, θ) be the cartesian and polar coordinates in the plane. The shape of the finger is the solution to the system of first order differential equations:

$$\begin{aligned} \dot{x} &= \mathcal{F}_x \\ \dot{y} &= \mathcal{F}_y \end{aligned} \tag{1}$$

where $\mathcal{F} = (\mathcal{F}_x, \mathcal{F}_y)$ is the vector field obtained in Section 3.2. The identity in Equation 2 relates the derivatives of cartesian and polar coordinates:

$$\frac{dy}{dx} = \frac{r' \sin\theta + r\cos\theta}{r'\cos\theta - r\sin\theta} \tag{2}$$

where $r' = \frac{dr}{d\theta}$. With it, we can rewrite the cartesian system 1 as the single polar differential equation:

$$\frac{\mathcal{F}_y}{\mathcal{F}_x} = \frac{r' \sin\theta + r\cos\theta}{r'\cos\theta - r\sin\theta} \tag{3}$$

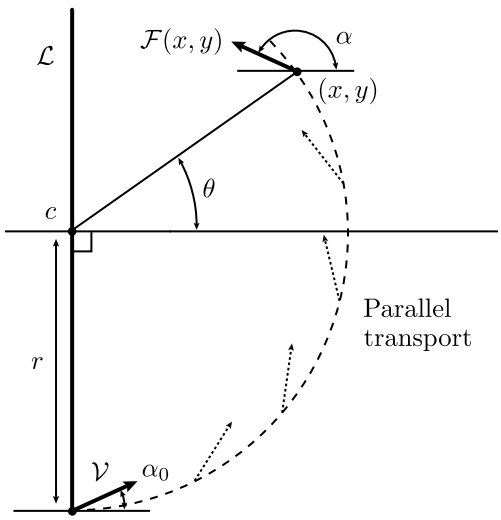

Figure 8: Normalized diagram for Case I: The parallel transport of $\mathcal{V}$ along an arc with center c gives us $\mathcal{F}(x,y)$, the direction of the vector field at (x,y), $\alpha = \alpha_0 + \theta + \frac{\pi}{2}$.

Without loss of generality we normalize the geometry of the problem and suppose that the contact curve $\mathcal{L}$ is parallel to the Y axis and the center of rotation c lies on the X axis. Let α_0 be the constant angle between $\mathcal{L}$ and the contact vector $\mathcal{V}$. Depending on the relative location of c and $\mathcal{L}$ we distinguish three cases that we will analyze separately in the next three sections:

i. The rotation center c lies on top of $\mathcal{L}$.

ii. The rotation center c is at finite distance from $\mathcal{L}$.

iii. The rotation center c is at infinity, i.e. the finger translates rather than rotates.

4.1 Case I: Rotation Center On the Contact Curve

In this case the distance between the center of rotation of the finger c and the contact curve $\mathcal{L}$ is zero. We place the origin of coordinates at c and the axis Y along the contact curve, as in Figure 8. In this case, Equation 3 becomes:

$$\frac{\mathcal{F}_y}{\mathcal{F}_x} = \tan\left(\alpha_0 + \theta + \frac{\pi}{2}\right) = \frac{r' \sin\theta + r\cos\theta}{r'\cos\theta - r\sin\theta} \tag{4}$$

Solving Equation 4 for r' yields:

$$r' = \frac{dr}{d\theta} = -r\tan\alpha_0 \tag{5}$$

Equation 5 is a linear homogeneous ordinary differential equation with solution:

$$r(\theta) = \mathrm{C}\ e^{-\theta\tan\alpha_0} \tag{6}$$

The solution to the invariant contact problem for case I is a logarithmic spiral with pitch $\frac{\pi}{2} + \tan^{-1}(\cot\alpha_0)$, which we could have anticipated from Figure 8 where the angle between the contact vector and the radial line (line from origin to the finger) is constant. This is

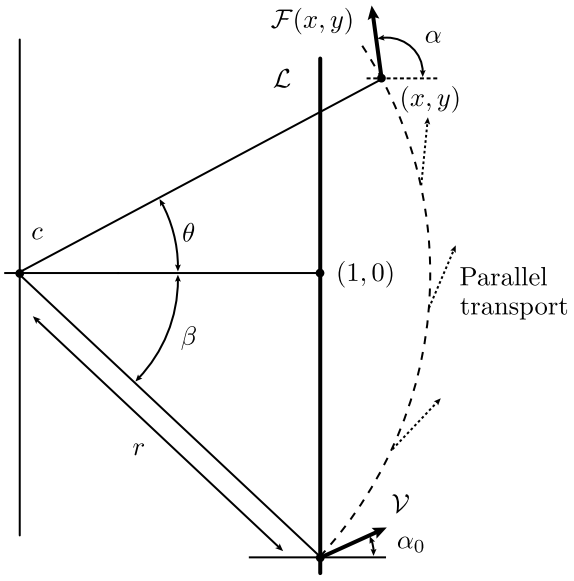

Figure 9: Normalized diagram for Case II: The parallel transport of $\mathcal{V}$ along an arc with center c gives us $\mathcal{F}(x,y)$, the direction of the vector field at (x,y), $\alpha = \alpha_0 + \theta + \beta$.

characteristic of logarithmic spirals and gives them their scale invariant properties [15], as we will further see in Section 6.

Notice that when the angle α_0 reaches one of the limit values $\pm\frac{\pi}{2}$, the logarithmic spiral becomes a straight line. This is caused by the contact vector becoming parallel to the contact line.

4.2 Case II: Rotation Center at Finite Distance from Contact Curve

In this case the rotation center c is at finite distance from the contact line $\mathcal{L}$. Without loss of generality we can scale the geometry of the problem so that the distance is unity. As in the previous case, we place the origin of coordinates at c. Now the contact line is vertical and crosses the X axis at $(1,0)$, as in Figure 8.

Equation 3 particularized to the construction in Figure 9 yields:

$$\frac{\mathcal{F}_y}{\mathcal{F}_x} = \tan\left(\alpha_0 + \theta + \beta\right) = \tan\left[\alpha_0 + \theta + \cos^{-1}\left(\frac{1}{r}\right)\right] = \frac{r'\sin\theta + r\cos\theta}{r'\cos\theta - r\sin\theta} \tag{7}$$

After some trigonometric algebra, Equation 7 can be solved for r' as:

$$r' = \frac{dr}{d\alpha} = r \cdot \frac{\cos\alpha_0 - \sqrt{r^2-1}\sin\alpha_0}{\sin\alpha_0 + \sqrt{r^2-1}\cos\alpha_0} \tag{8}$$

Equation 8 is a separable differential equation with form $\frac{dr}{d\theta} = g(r)$, which can be solved as

$\theta(r) = \int d\theta = \int \frac{1}{g(r)} dr$, with the change of variables $t \to \sqrt{r^2-1}$:

$$\begin{aligned}
\theta(r) &= \int \frac{1}{r} \cdot \frac{\sin\alpha_0 + \sqrt{r^2-1}\cos\alpha_0}{\cos\alpha_0 - \sqrt{r^2-1}\sin\alpha_0}\, dr = \\
&= \int \frac{t}{t^2+1} \cdot \frac{(\sin\alpha_0 + t\cos\alpha_0)}{(\cos\alpha_0 - t\sin\alpha_0)}\, dt = \\
&= -\int \frac{1}{t^2+1} + \frac{\cos\alpha_0}{\sin\alpha_0 t - \cos\alpha_0}\, dt = \\
&= -\tan^{-1}(t) - \frac{\ln\left(|\sin\alpha_0 t - \cos\alpha_0|\right)}{\tan\alpha_0}
\end{aligned} \tag{9}$$

As illustrated in Figure 10, Equation 9 yields the α_0-parametrized family of spirals:

$$\theta(r) = -\tan^{-1}\left(\sqrt{r^2-1}\right) - \frac{\ln\left(|\sin\alpha_0\sqrt{r^2-1} - \cos\alpha_0|\right)}{\tan\alpha_0} + \mathrm{C} \tag{10}$$

The solution is valid for all possible values of α_0 except when $\tan\alpha_0 = 0$, in which case a similar derivation yields:

$$\theta(r) = -\tan^{-1}\left(\sqrt{r^2-1}\right) + \sqrt{r^2-1} + \mathrm{C} \tag{11}$$

4.3 Case III: Rotation Center at Infinity

In this case the center of rotation c is located at infinity. This is equivalent to a translating finger, i.e., the finger joint is prismatic rather than revolute.

The vector field $\mathcal{F}$ is in this case generated by the parallel transport of the contact curve and contact vector along parallel lines oriented with the direction of translation. The obtained vector field is independent of the direction of translation: $\mathcal{F}$ is constant across the entire plane and oriented with α_0 except in the singular case when the direction of translation is parallel to the contact line. In this case the vector field is only defined on top of the contact line.

The integral curve of $\mathcal{F}$ is always a line segment aligned with the constant contact vector $\mathcal{V}$, which yields straight fingers. In the degenerate situation of the direction of translation being aligned with the contact line, the solution only exists if the contact vector is also aligned with the contact line, in which case the integral curve is also a straight line segment.

4.4 Family of Solutions

In cases I and II, the integral curve of the vector field is a spiral, with the exception of a few degenerate situations where the integral curve is either a line segment or a circle. We make special note of case I with $\alpha_0 = 0$ where the contact vector is perpendicular to the contact line. This produces an impractical circular finger that only meets one of the constraints, while, at the same time, does not violate any of the rest.

In case III, we always obtain a line segment. Figure 10 shows a summary of the solutions for different values of α_0. Note that the vector fields obtained with α_0 and $\alpha_0 + \pi$ always have the same magnitude and opposite direction, hence it suffices to analyze the range $\left[\frac{\pi}{2}, -\frac{\pi}{2}\right]$. In Figure 10 we show a long section of the spiral. However, for practical reasons, the actual shape of the finger is just a small portion.

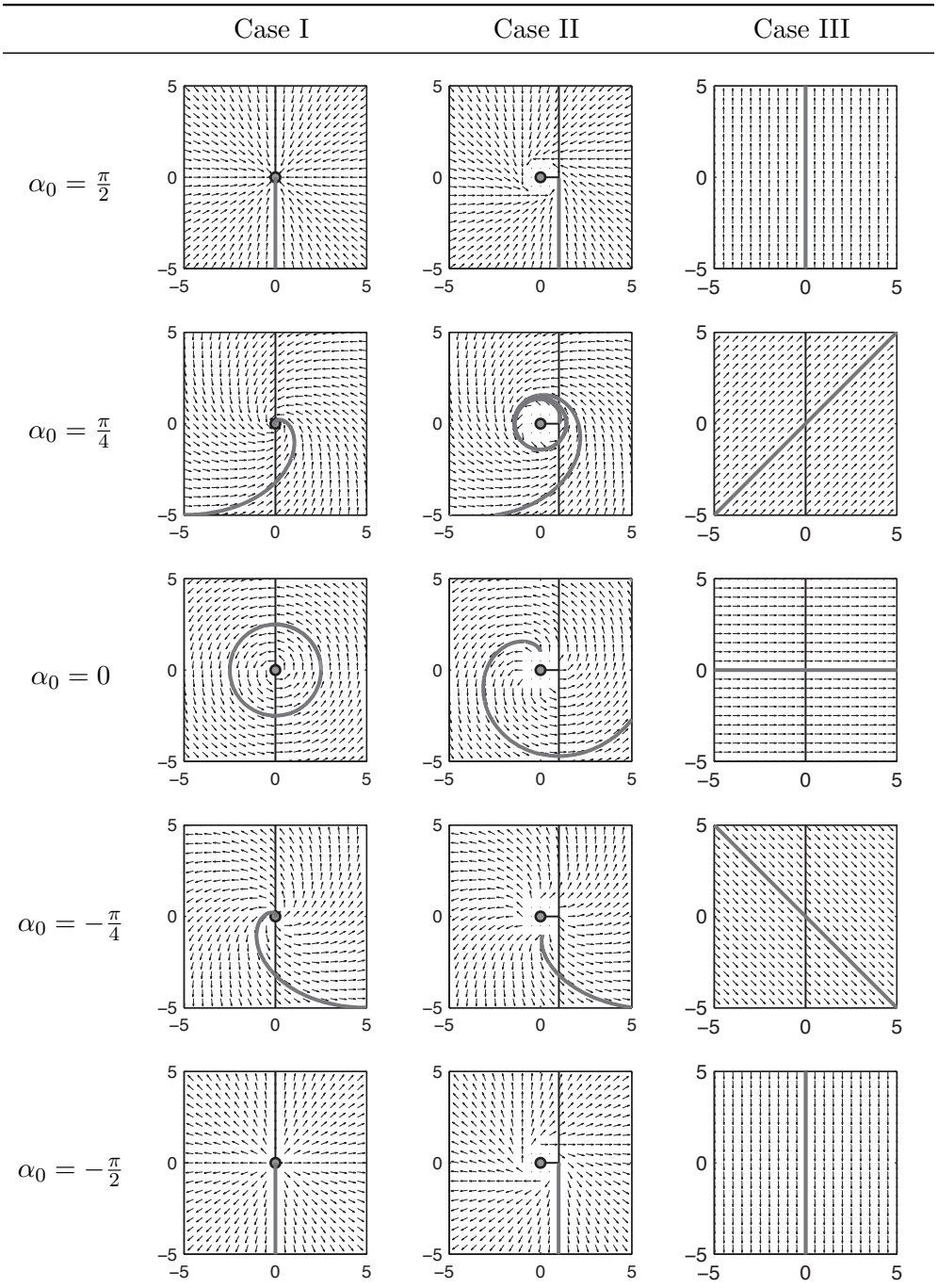

Figure 10: Plots show the contact curve (*vertical bold line*), the rotation center (*grey dot*), and the finger solution (*grey curves*) for different values of α_0. The finger always crosses the lower half of the contact curve with constant angle α_0. Case I: Rotation center on the contact curve. Case II: Rotation center at finite distance from the contact curve. Case III: Rotation center at infinity.

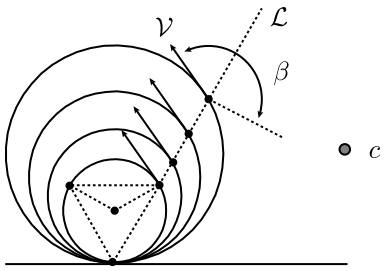

(a)

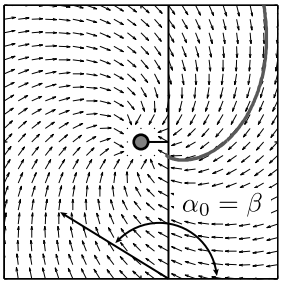

(b)

Figure 11: (a) Contact curve $\mathcal{L}$ and contact vector $\mathcal{V}$ of the fingers of a scale invariant gripper. (b) Corresponding normalized diagram, where $\alpha_0 = \beta$.

5 Applications to Grasping

In this section we apply the grasp invariance principle to design fingers of grasping hands. We give examples with both scale and pose transformations.

5.1 Scale Invariant Grasping

The solution to the scale-invariant contact problem in Figure 1 yields a finger with invariant contact geometry for a disk of varying size. Two such add up to a gripper whose equilibrium grasps are geometrically invariant with scale. Suppose we aim for a triangular grasp between two fingers and a palm. Figure 11a shows the corresponding contact line $\mathcal{L}$ and contact vector $\mathcal{V}$. After the normalization of the geometry proposed in Section 4, we get the diagram in Figure 11b. The solution belongs to the family of spirals obtained in Case II in Section 4.2, where the center of rotation is at finite distance from the contact line.

The contact line, the contact vector, and the form of the finger depend on the object O and the type of contact we aim for. Therefore, the form of the finger depends on the task to solve. For the specific example of a disk and the triangular grasp in Figure 11a, we can construct a scale-invariant gripper by combining two identical but symmetric fingers as in Figure 12.

5.2 Pose Invariant Grasping

Here we aim to design a hand whose grasps are invariant with respect to the location of a given object rather than scale. Suppose again that we want to grasp a disk of a given size with a triangular grasp, against a planar palm. Now, the disk can be located anywhere along

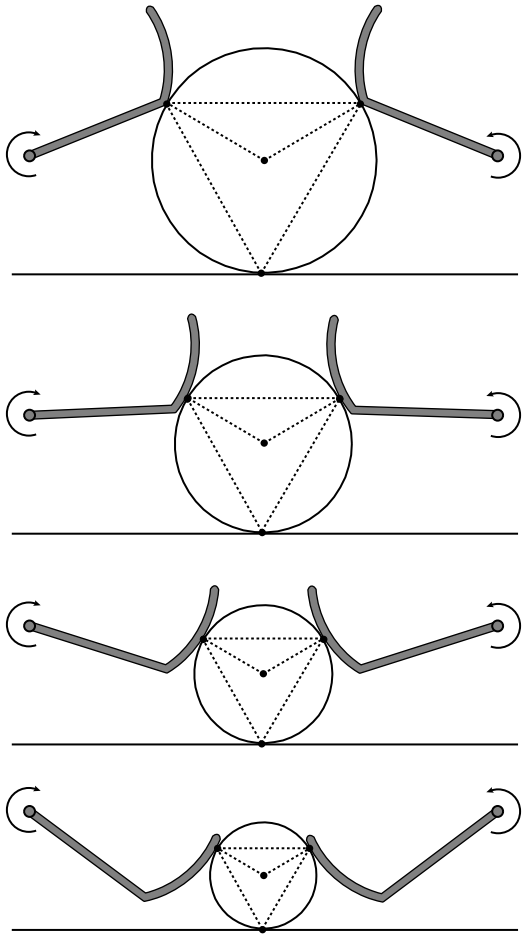

Figure 12: Gripper with scale invariant fingers for grasping disks with a triangular grasp.

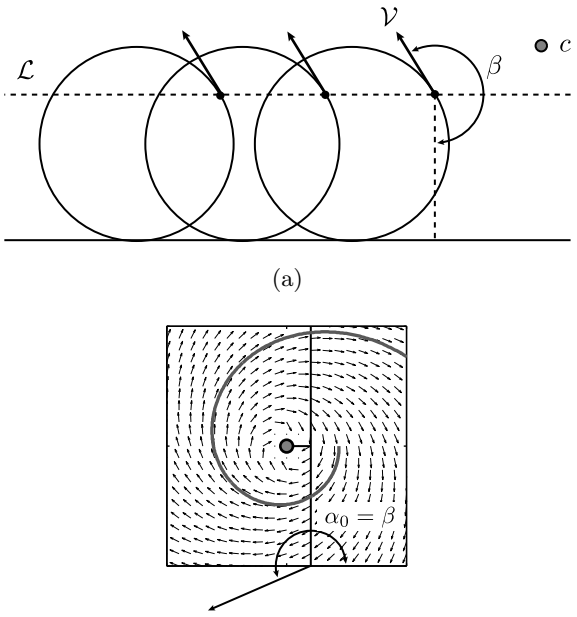

Figure 13: (a) Contact curve $\mathcal{L}$ and contact vector $\mathcal{V}$ of the fingers of a pose invariant gripper. (b) Corresponding normalized diagram, where $\alpha_0 = \beta$.

the palm, and we want the grasp geometry to be invariant with respect to that displacement. Figure 13a shows the corresponding contact line $\mathcal{L}$ and contact vector $\mathcal{V}$, and Figure 13b shows the corresponding normalized diagram. Since the rotation center is at finite distance from the contact line, the solution belongs to the family of spirals in Case II in Section 4.2.

Again, the contact line, the contact vector and consequently the form of the finger depend on the object O and the type of contact desired. In Figure 14 two identical but symmetric fingers compose a pose-invariant gripper.

5.3 Pick-up Tool

Suppose we are to design a gripper with two rigid fingers to pick up an object from the ground. The object needs to slide along the length of the fingers while it is being lifted, similar to Trinkle and Paul's work on dexterous manipulation with sliding contacts [17]. Because of the critical role that contact geometry plays in the sliding motion, complex lift plans can be simplified if the contact geometry between finger and object were to be invariant with respect to the lifting motion. With that in mind, we can use the grasp invariance principle to find the finger shape that preserves a contact suitable for sliding. Figure 15 shows a gripper designed to pick up disks.

6 Applications to Common Devices

In this section we apply the grasp invariance principle to derive optimal shapes for three common devices: a rock-climbing cam, an anti kickback device for table saws and a jar wrench.

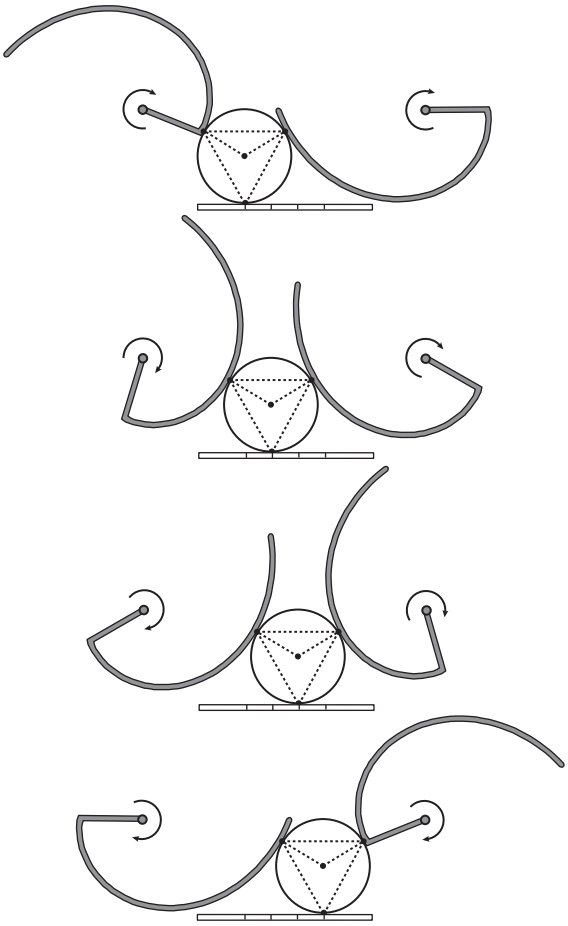

Figure 14: Gripper with location invariant fingers for grasping disks with a triangular grasp.

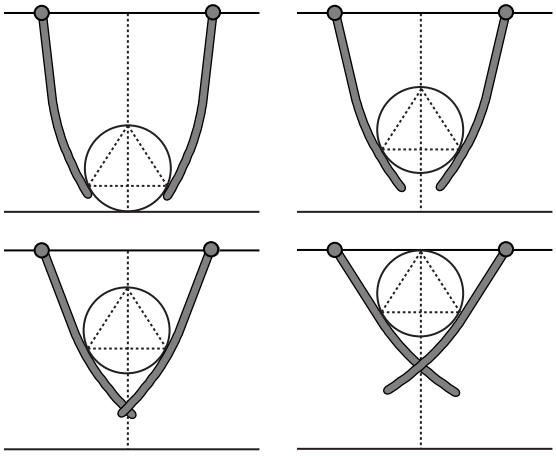

Figure 15: Invariant contact geometry of the pick-up tool when lifting an object from the ground.

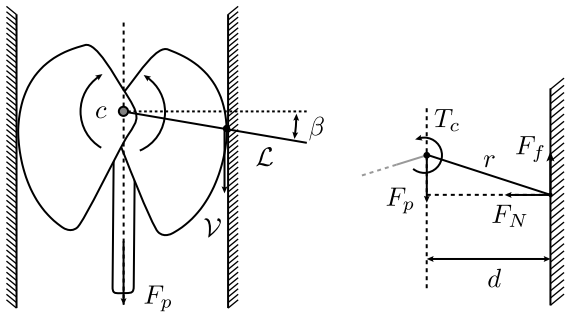

(a) (b)

Figure 16: (a) Spring loaded cam for rock-climbing. (b) Static force diagram.

6.1 Rock-Climbing Cam

A spring loaded cam is a safety device used in rock climbing to secure anchor points in cracks in the rock face. The device uses the mechanical advantage of the wedge effect to convert pulling force into huge friction forces, (Figure 16a). That conversion depends on the coefficient of friction of the wall μ and the cam angle β. From the diagram on Figure 16 (b) the condition for static equilibrium (zero torque at rotation center c) is:

$$\begin{aligned} & r \cdot F_f \cos\beta = r \cdot F_N \sin\beta \\ [F_f \leq \mu F_N] \qquad & F_N \tan\beta \leq \mu F_N \\ & \beta \leq \tan^{-1}\mu \end{aligned} \tag{12}$$

where r is the distance from the cam rotation center c to the contact point, F_N is the normal force caused as a reaction to the pulling force F_p, and F_f is the frictional force. For a cam to have a loading pattern invariant with the size of the crack it needs to preserve the contact angle β while the cam opens and closes to adapt to different wall widths.

Each wall width imposes a tangential constraint on the form of the cam. We can apply the invariant contact principle to derive a shape for the cam so that β remains constant despite variations in d. The rotation center lies on top of the contact line $\mathcal{L}$, hence the solution is a logarithmic spiral with $\alpha_0 = \beta$ (Case I in Section 4.1) as shown in Figure 17.

The logarithmic spiral has been used for decades in the design of climbing cams. The invention of modern rock-climbing cams is attributed to Raymond Jardine [11]. His invention used a logarithmic spiral, with camming angle $\beta = 13.5°$.

6.2 Anti Kickback Device for Table Saws

Table saw kickback happens when the blade catches the workpiece and violently throws it back to the front of the saw, towards the operator. An anti kickback device is a passive device that only allows forward motion of the workpiece. Among several options to introduce the asymmetry, one option is to use a spiral like rotating part that wedges a workpiece trying to move backwards, (Figure 18a).

Experimental studies have determined that the optimal contact between the workpiece and the anti kickback device is reached when $\beta = 8°$ [2]. To make the contact invariant with the

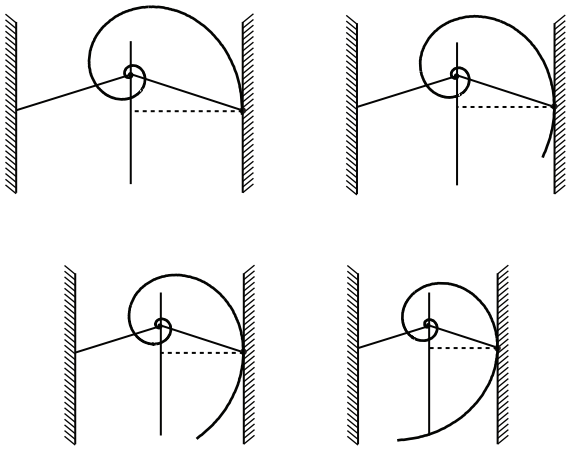

Figure 17: Invariant loading pattern for different wall openings when using a logarithmic spiral profile for the cam.

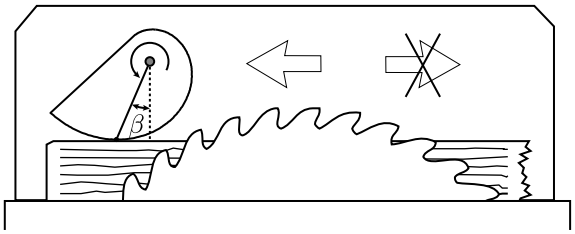

(a)

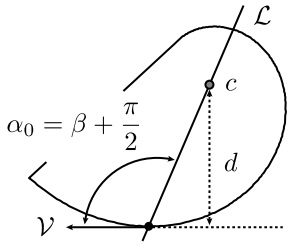

(b)

Figure 18: (a) Anti kickback device as used in a wood table saw. (b) The contact between the retaining part and the workpiece is at an optimum angle β.

thickness of the workpiece, we can use the grasp invariance principle to design the shape of the device. The center of rotation lies on top of the contact line $\mathcal{L}$ and consequently the optimal solution is a logarithmic spiral, with $\alpha_0 = \beta + \frac{\pi}{2}$, as shown in Figure 21. The patent of the device [2] proposed a logarithmic spiral as the optimal contour.

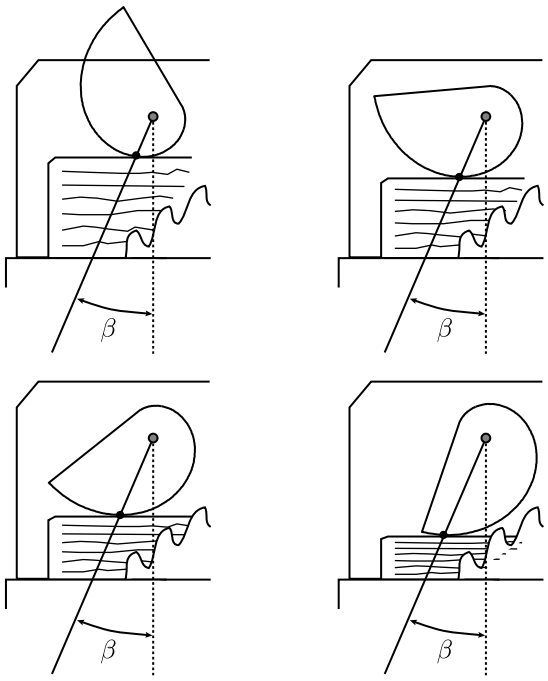

Figure 19: Invariant contact geometry for different workpiece thicknesses when using a logarithmic spiral from for the anti kickback device.

6.3 Jar Wrench

The jar wrench in Figure 2b opens jars of varying sizes. Figure 20a shows the basic operating principle. The lid contacts the inner disk and the outer contour at different places for different sized lids. The mechanics of the opening procedure, and specifically the amount of friction available, depends on the value of the angle β.

If we know the optimal value of β, and want the mechanics to be invariant across the range of jar lid sizes, we can use the grasp invariance principle to design the contour. To simplify the analysis we suppose, as shown in Figure 20b, that the lids are fixed and resting always against the same contact point, while the wrench rotates to contact the lid. The center of rotation is on top of the contact line $\mathcal{L}$, consequently the optimal shape of the jar wrench is a logarithmic spiral, with $\alpha_0 = \frac{\pi}{2} - \beta$.

7 Discussion

In this paper we introduce the grasp invariance principle and provide a recipe to apply it to the design of rotating fingers and fixtures. Given a continuum of shape or pose variation and a

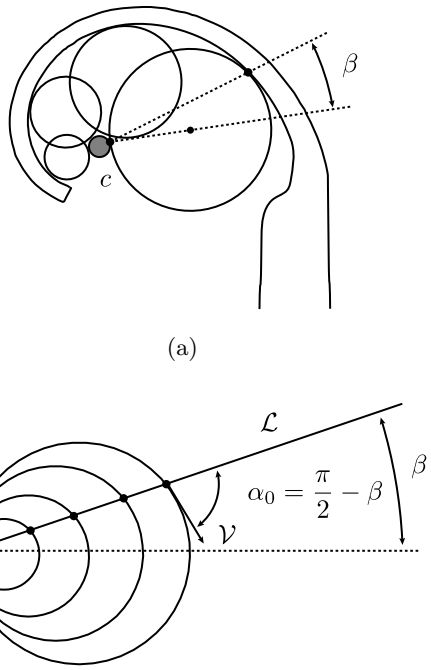

Figure 20: (a) Jar wrench. (b) Simplified diagram where the discs are fixed and the wrench rotates.

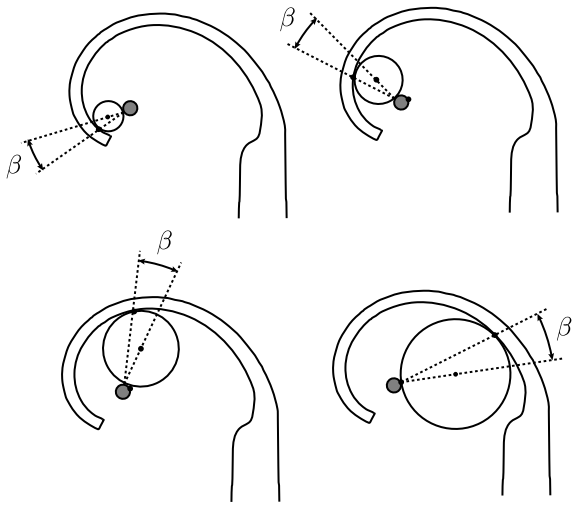

Figure 21: Invariant contact geometry for different sized lids.

property to be held invariant we derive an optimal shape that satisfies the property across the continuum. We have shown that, in simple cases, the finger has a spiral form, and have applied the technique to design scale-invariant and pose-invariant grippers for disks and a pick-up tool. Finally we have analyzed the shape of a few common devices under the principle.

There are lots of extensions, generalizations and applications that we wish to explore. Here we mention a few of them:

- Open design questions: Where should we put the center of rotation c? How do we choose the transformation $\mathcal{H}(t, s)$? The finger shape depends both on c and $\mathcal{H}(t, s)$. Those parameters can be chosen to satisfy additional properties. Specially we are interested in the possibility of optimizing the location of c so as to avoid the interpenetration constraints mentioned in Section 3.3.

- This paper covers design issues of rotating and prismatic fingers. There are other types of finger motion worth considering, for example those involving linkages.

- 2D designs are readily adapted to design grasp invariant 3D grippers, for example by arranging three fingers symmetrically around a circular palm. However we can also think about a deeper 3D generalization where the contact vector becomes the contact hyperplane and fingers become 2D surfaces.

- What happens when we deal with non-smooth boundaries? Can we extend the approach to include contact at vertices?

- The grasp invariance principle applies to one-dimensional variations of shape or pose of the object, e.g. scale-invariant or pose-invariant grippers. How can we trade off various objectives to address generalization across objects and tasks?

- Grasp invariance is both a principle and a method. The same method in Section 3.2 can also be applied to synthesize grasp variance, where different objects are grasped differently.

- In this paper we have focused on the design of fingers, however the same principle can be applied to the design of feet. Curved shaped feet have the potential to provide robustness with respect to variations in the terrain.

Acknowledgments

We wish to thank Garth Zeglin, Siddhartha Srinivasa, Amir Degani, Ross Knepper and Tomas Simon for discussions, comments and insights.

This work was supported by the National Science Foundation [NSF-IIS-0916557], the Defense Advanced Research Projects Agency [DARPA-BAA-10-28] and Army Research Laboratory [W911NF-10-2-0016]. This work does not necessarily reflect the position or the policy of the U.S. Government, DARPA or ARL. No official endorsement should be inferred.

References

[1] Barret Technologies: The Barret hand, 2001.

[2] J. Berkeley. Anti-Kickback System, 1986.

[3] R.-P. Berretty, K. Goldberg, M. H. Overmars, and A. F. van der Stappen. On Fence Design and the Complexity of Push Plans for Orienting Parts. In *Symposium on Computational Geometry (SCG)*, pages 21–29, 1997.

[4] R.-P. Berretty, K. Goldberg, M. H. Overmars, and A. F. van der Stappen. Trap Design for Vibratory Bowl Feeders. *International Journal of Robotics Research*, 20(11):891–908, 2001.

[5] A. Bicchi and V. Kumar. Robotic Grasping and Contact: A Review. In *IEEE International Conference on Robotics and Automation (ICRA)*, pages 348–353. Ieee, 2000.

[6] M. Brokowski, M. Peshkin, and K. Goldberg. Optimal Curved Fences for Part Alignment on a Belt. *Journal of Mechanical Design*, 117(1):27–35, 1995.

[7] J. Butterfass, M. Grebenstein, H. Liu, and G. Hirzinger. DLR-Hand II: Next Generation of a Dextrous Robot Hand. In *IEEE International Conference on Robotics and Automation (ICRA)*, pages 109–114, 2001.

[8] M. R. Cutkosky. On Grasp Choice, Grasp Models, and the Design of Hands for Manufacturing Tasks. *IEEE Transactions on Robotics and Automation*, 5(3):269–279, June 1989.

[9] A. M. Dollar and R. D. Howe. Joint Coupling Design of Underactuated Grippers. In *30th Annual Mechanisms and Robotics Conference*, pages 903–911. Harvard University, 2006.

[10] A. M. Dollar and R. D. Howe. The Highly Adaptive SDM Hand: Design and Performance Evaluation. *The International Journal of Robotics Research*, 29(5):585–597, Feb. 2010.

[11] R. Jardine. Climbing Aids, 1980.

[12] M. Peshkin and A. Sanderson. Planning Robotic Manipulation Strategies for Workpieces that Slide. *IEEE Journal on Robotics and Automation*, 4(5):524–531, 1988.

[13] A. Rodriguez, M. T. Mason, and S. S. Srinivasa. Manipulation Capabilities with Simple Hands. In *International Symposium on Experimental Robotics (ISER)*, 2010.

[14] D. A. Theobald, W. J. Hong, A. Madhani, B. Hoffman, G. Niemeyer, L. Cadapan, J.-J. Slotine, and J. K. Salisbury. Autonomous Rock Acquisition. In *AIAA Forum on Advanced Developments in Space Robotics*, 1996.

[15] D. W. Thompson. *On Growth and Form.* Cambridge University Press, 1961.

[16] J. A. Thorpe. *Elementary Topics in Differential Geometry.* Springer, 1979.

[17] J. Trinkle and R. Paul. Planning for Dexterous Manipulation with Sliding Contacts. *International Journal of Robotics Research*, 9(3):24–48, 1990.

[18] N. T. Ulrich. Grasping with Mechanical Intelligence, 1989.

[19] N. T. Ulrich, R. Paul, and R. Bajcsy. A Medium-Complexity Compliant End Effector. In *IEEE International Conference on Robotics and Automation (ICRA)*, pages 434–436, 1988.

[20] D. E. Whitney, R. E. Gustavson, and M. P. Hennessey. Designing Chamfers. *International Journal of Robotics Research*, 2(4):3–18, 1983.

[21] J. Wiegley, K. Goldberg, M. Peshkin, and M. Brokowski. A Complete Algorithm for Designing Passive Fences to Orient Parts. *Assembly Automation*, 17(2):129–136, 1997.

[22] M. T. Zhang and K. Goldberg. Gripper Point Contacts for Part Alignment. *IEEE Transactions on Robotics and Automation*, 18(6):902–910, Dec. 2002.